Short Communication

Rapid electrochemical characterization of battery electrode materials in the solid state

D.A. Fiedler [a,*], J.O. Besenhard [a], M.H. Fooken [b]

[a] Institut für Chemische Technologie Anorganischer Stoffe, Technische Universität Graz, Stremayrgasse 16/III, 8010 Graz, Austria
[b] Riedel-de Haën AG, 30926 Seelze, Germany

Abstract

Battery electrode materials such as $Li_xMn_2O_4$ and γ-MnO_2 are characterized in the solid state by cyclic voltammetry when mechanically attached to an electrode surface. At voltammetric scan rates in the mV/s range, identical peak potentials and essentially the same peak shapes are observed when compared with voltammograms recorded at conventional composite electrodes at scan rates in the μV/s range. The method provides a convenient tool for the rapid screening of battery electrode materials. © 1997 Published by Elsevier Science S.A.

Keywords: Electrodes; Lithium; Manganese; Cyclic voltammetry; Solid-state electrochemistry; Batteries

1. Introduction

Battery electrode materials are commonly characterized by electrochemical methods such as cyclic voltammetry and chronopotentiometry [1]. Cyclic voltammetry is a powerful tool for probing kinetic and thermodynamic properties of the compound studied. The peak shape and the number of observable redox processes within a given potential range may provide additional criteria for the selection of a proposed battery electrode material. Electrode 'cycling' or multiple double-step chronopotentiometry is then applied to promising compounds in order to obtain information regarding the available capacity and possible cycle life of an electrode. Consequently, voltammetric techniques are initially valuable in order to discriminate between 'good' and 'bad' battery electrode materials. However, commonly employed composite or thin-film electrodes are not only defined by the active electrode material, but also by the electrode porosity or additives such as binders and conductivity enhancers. Required voltammetric scan rates are typically in the μV/s range in order to compensate for slow mass-transfer processes which occur mainly due to the porosity of such an electrode.

Recent advancements in electroanalytical techniques [2,3] allow the voltammetric characterization of solid materials when attached to an electrode surface. Voltammetry at single particles at fibrous micro-electrodes [2] has been reported

very recently. At single particles, no broadening of the voltammetric signals due to particle size distribution would be expected. Consequently, cyclic voltammograms exhibit symmetric, well-defined peaks resembling those observed at thin homogeneous films. Depending on the particle size and transport properties of the material with respect to incorporated ions, voltammetric scan rates in the mV/s range can be achieved. While single particles can thus be analysed very elegantly and rapidly, experimental conditions are far from those in a compositional battery electrode. However, a different technique was also recently introduced by Scholz et al. [3] which allows ensembles of micro-crystalline particles to be analysed electrochemically. Micro-crystalline compounds are mechanically attached to the surface of a conventional disk-shaped electrode by virtually polishing the electrode with the compound to be studied, causing some particles to adhere to the electrode surface. Studies at rotating electrodes [4] showed the micro-crystals to adhere even under conditions of forced convection. The individual conductivity of the sample compound does not affect the voltammetric behaviour [4]. This method should therefore be advantageous when studying poorly conductive battery electrode materials such as manganates and manganese oxides. The maximum applicable scan rate without loss of thermodynamic information is expected to depend mainly on the transport kinetics within the solids, since any effects of porosity and additives are avoided. However, effects due to a distribution of particle size are expected to result in broadened voltammetric signals.

* Corresponding author. Tel.: +43-316-873 8288; Fax: +43-316-873 8272; e-mail: F537DIRK@MBOX.TU-GRA2.AC.AT

Spinel-type $Li_xMn_2O_4$, $0.9 \leq x \leq 1.1$, and γ-MnO_2 were used as typical examples of battery materials which are used in the positive electrodes of, e.g. lithium ion and zinc/manganese dioxide rechargeable batteries [5], respectively. Cyclic voltammograms of the compounds when attached mechanically to the surface of glassy carbon and platinum disk electrodes are compared with those reported for composite electrodes.

2. Experimental

$Li_xMn_2O_4$, $0.9 \leq x \leq 1.1$ (Riedel–de Haën, Germany) and γ-MnO_2 (Toyo Soda Hellinica, Greece) were used as received. For investigations of $Li_xMn_2O_4$, a solution of 1 M $LiClO_4$ (Aldrich, Germany) in a 1:2 mixture of ethylene carbonate (Merck, Germany) and dimethyl carbonate (Merck, Germany) was used under argon atmosphere. The auxiliary and reference electrodes were pieces cut from battery grade lithium foil. γ-MnO_2 was studied in freshly prepared and argon-saturated aqueous solutions of 9 N KOH using a platinum mesh auxiliary electrode and a Hg/HgO/9 N KOH reference electrode. Either a 3 mm diameter glassy carbon disk or a 0.5 mm platinum disk working electrode completed the three-electrode arrangement. The glassy carbon working electrode was polished and cleaned with SiC paper (#1000, 18.3 μm, Struers, Denmark). The platinum disk electrode was polished with 1 μm diamond paste (Struers, Denmark) prior to being used. The compound to be studied was placed on a sheet of white paper and transferred to the electrode surface by rubbing firmly the electrode on the solid material as illustrated in Fig. 1. Both uncovered glassy carbon and platinum working electrodes were electrochemically inactive under the conditions applied. Cyclic voltammograms were recorded using the IM6 software package running on an IM5d system (all Zahner Elektrik, Germany).

3. Results and discussion

3.1. $Li_xMn_2O_4$

The shape and peak potentials of cyclic voltammograms of $Li_xMn_2O_4$ recorded at a scan rate of 10 mV/s (Fig. 2)

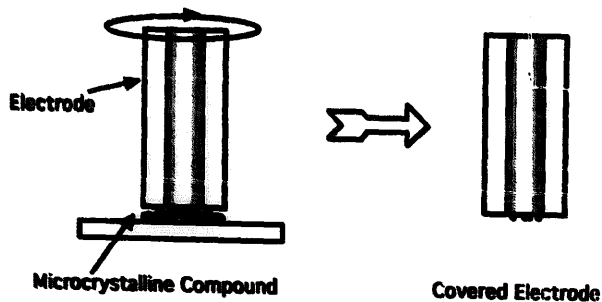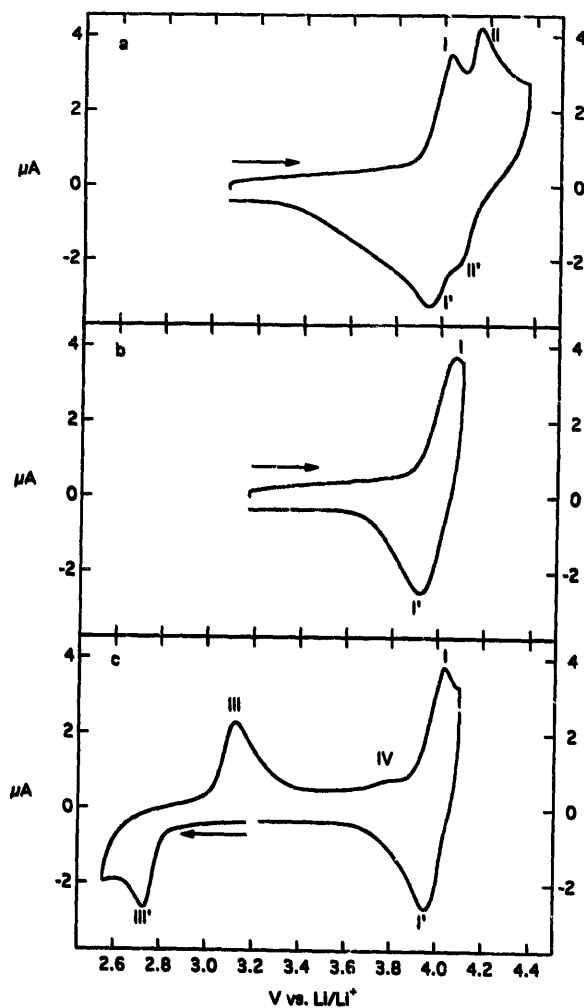Fig. 1. Mechanical attachment of solid micro-crystalline particles to a disk electrode.

Fig. 2. Cyclic voltammetry of $Li_xMn_2O_4$ mechanically attached to a 3 mm diameter glassy carbon disk electrode. Ethylene carbonate:dimethyl carbonate = 1:2 (1 M $LiClO_4$). Li/Li⁺ reference electrode. Scan rate: 10 mV/s, sweep start and direction as indicated by arrows. (a) and (b) oxidation processes, and (c) reduction and oxidation processes, sweep immediately following that shown in (b).

agree entirely with those reported earlier for composite [6] and thin film [7] electrodes, which were recorded at a scan rate of 100 μV/s. Values of peak and half-wave potentials are compared with published data [8] in Table 1. The exhaustive oxidation of $Li_xMn_2O_4$ is accompanied by loss of Li^+ ions and proceeds via two processes I/I' and II/II' at $E_{1/2}$ values of 3.98 and 4.10 V versus Li^+/Li, respectively (Fig.

Table 1

Voltammetric data of $Li_xMn_2O_4$ at a 3 mm diameter glassy carbon disk electrode in ethylene carbonate:dimethyl carbonate = 1:2 (1 M $LiClO_4$) and comparison with data from Ref. [6] for a composite electrode; potentials vs. Li/Li⁺ reference electrode

Process	E_p (this work) (V)	$E_{1/2}$ (V)	$E_{1/2}$ ([6]) (V)
I/I'	4.03/3.94	3.98	4.01
II/II'	4.16/4.04	4.10	4.15
III/III'	3.13/2.73	2.93	2.97
IV	3.80		

2(a)). Switching the potential after process I (Fig. 2(b)) clearly shows that processes I/I′ and II/II′ occur independently. While process I/I′ corresponds to the formation of a solid solution of two cubic Mn(III) and Mn(IV) oxide phases, process II/II′ is due to phase mixing [8]. Prior to transformation of $Li_xMn_2O_4$ to $Li_2Mn_2O_4$ at $E_{1/2} = 2.93$ V versus Li^+/Li, process III/III′, results in slightly narrower signals in the oxidation region (Fig. 2(c)). The irreversible process IV at 3.80 V versus Li^+/Li (Fig. 2(c)) was shown to be a consequence of process III/III′ [8]. The reduction process III′ leading to $Li_2Mn_2O_4$ is known to result in a 5%-lattice expansion which results in mechanical decomposition of composite electrodes [8]. However, when micro-crystalline $Li_xMn_2O_4$ is reduced when mechanically attached to an electrode surface, no loss of material is evident as judged by the similar peak currents of subsequently recorded voltammograms at the same electrode (Fig. 2(b) and (c)). Cyclic voltammograms of micro-crystalline $Li_xMn_2O_4$ when attached to an electrode surface thus provide within minutes essentially the same amount of qualitative information as those recorded at composite electrodes within hours.

3.2. γ-MnO₂

The shape and peak potentials of cyclic voltammograms of γ-MnO₂ recorded at a scan rate of 2 mV/s (Fig. 3) agree with data of composite electrodes recorded at 25 μV/s [9]. Values of peak potentials are compared with published data [9] in Table 2. The homogeneous solid-state reduction of γ-MnO₂ to MnOOH in the potential region 0.2 to −0.3 V versus Hg/HgO/9 N KOH [9] takes place through two ill-defined processes V′ and VI′ (Fig. 3(a) and (b)) which are controlled by the simultaneous uptake of electrons and protons [10]. Reversible re-oxidation to γ-MnO₂ also results in broad signals as reported earlier [9]. Upon cycling to more negative potentials (Fig. 3(c)), the well-defined diffusion-limited process VII′, as judged by the peak shape, appears at a peak potential of −0.44 V versus Hg/HgO/9 N KOH. However, the observed peak current ratio of $i_{p,VII'}/i_{p,VI'} \approx 2$ is in contradiction to that found at composite electrodes [9], $i_{p,VII'}/i_{p,VI'} \approx 0.5$, and is explained as follows. Process VII′ is attributed to the heterogeneous reduction of MnOOH via a dissolution/reduction/precipitation process [10]. Due to the electrode preparation technique in this work, a loose rather than a compressed assembly of γ-MnO₂ particles is exposed to the surrounding electrolyte solution. Relatively free diffusion of electrolyte constituents such as OH^- ions to the electrode surface thus enables thorough dissolution of electrochemically inactive MnOOH as $[Mn(OH)_6]^{3-}$ [10]. Subsequent electrochemical reduction at the platinum electrode through process VII′ then produces $[Mn(OH)_6]^{4-}$ which is less soluble than $[Mn(OH)_6]^{3-}$ and precipitates as $Mn(OH)_2$ on the electrode surface [10]. At composite electrodes, this mechanism is limited by the restricted solubility of $[Mn(OH)_4]^-$ in the electrolyte solution within the electrode pores. Furthermore, electrochemical reduction can only
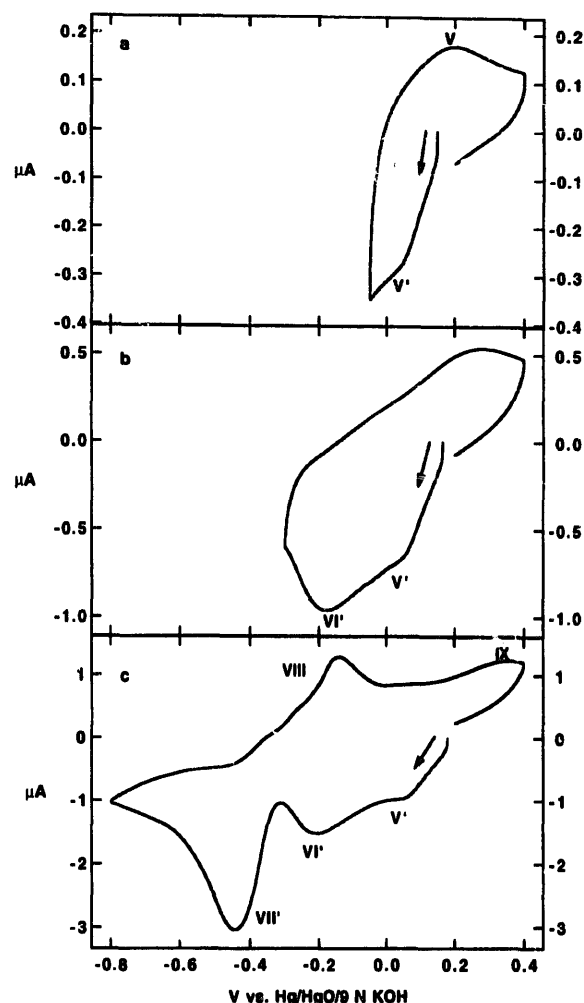

Fig. 3. Cyclic voltammetry of γ-MnO₂ mechanically attached to a 0.5 mm diameter platinum disk electrode, 9 N KOH, Hg/HgO/9 N KOH reference electrode. Scan rate: 2 mV/s, sweep start and direction as indicated by arrows. (a) and (b) homogeneous phase reduction processes, and (c) homogeneous and heterogeneous reduction processes.

Table 2

Voltammetric data of γ-MnO₂ at a 0.5 mm diameter platinum disk electrode in 9 N KOH and comparison to data from Ref. [9] for a composite electrode. Potentials vs. Hg/HgO/9 N KOH reference electrode

Process	E_p (this work) (V)	E_p ([9]) (V)
V/V′	0.20/0.03	0.30/0.04
VI′	−0.20	−0.24
VII′	−0.44	−0.45
VIII	−0.14	−0.12
IX	0.28/0.35	0.20

take place at the conductive carbon particles of a composite electrode due to the insulating properties of MnOOH [10]. Dissolution of MnOOH and subsequent diffusion of dissolved $[Mn(OH)_4]^-$ thus limit the observable faradaic current to yield a rather ill-defined signal for process VII′ at a composite electrode. During the reverse sweep, oxidation of $Mn(OH)_2$ to Mn(III) species and finally MnO₂ is attributed

to processes VIII and IX, respectively [9]. Cyclic voltammograms of micro-crystalline γ-MnO$_2$ when mechanically attached to an electrode surface thus provide within minutes more detailed information than those recorded at composite electrodes within hours.

Applicable scan rates for the above technique should generally be well below 200 to 2 mV/s based on the following assumptions. The processes in the solids will be governed by a diffusion coefficient D of incoming or leaving ions in the range of $D = 10^{-9}$ to 10^{-11} cm^2/s [1,11] and the average particle size $d = 0.2$ μm as derived from scanning electron microscopy images of Li$_x$Mn$_2$O$_4$ and γ-MnO$_2$ employed in this work. With $d^2/(4Dt) \gg 1$ (time, t) [1], an estimate of the maximum time which is needed to reach equilibrium over a potential window of 20 mV yields the above values for the maximum applicable scan rate.

4. Conclusions

When mechanically attached to an electrode surface, battery electrode materials such as Li$_x$Mn$_2$O$_4$ and γ-MnO$_2$ have been shown to exhibit the same characteristic voltammetric behaviour for homogeneous electron-transfer processes as compared with composite electrodes. Applicable scan rates are in the mV/s range, effectively reducing the time scale required for the analysis of such materials from hours to minutes. Heterogeneous processes such as the dissolution/reduction/precipitation sequence during the exhaustive reduction of γ-MnO$_2$ result in well-defined voltammetric signals which provide more detailed information about the

nature of possible reaction pathways than those recorded at composite electrodes.

Acknowledgements

References

[1] C. Julien and G.-A. Nazri (eds.) in: "Solid State Batteries: Materials Design and Optimization", Kluwer, Dordrecht, The Netherlands, 1994.

[2] H. Ura, T. Nishina and I. Uchida, J. Electrochem. Soc., 396 (1995) 169; I. Uchida, H. Fujiyoshi and S. Waki, Ext. Abst., 8th Int. Meeting Lithium Batteries, Nagoya, Japan, 1996, p. 129.

[3] F. Scholz, L. Nitschke and G. Henrion, Naturwissenschaften, 76 (1989) 71; F. Scholz and B. Meyer, Chem. Soc. Rev., 23 (1994) 341; A.M. Bond and F. Scholz, J. Phys. Chem., 95 (1991) 7460.

[4] A.M. Bond and F. Marken, J. Electroanal. Chem., 372 (1994) 125; A.M. Bond and D.A. Fiedler, J. Electrochem. Soc., 144 (1997) 1566.

[5] J.O. Besenhard, Mater. Sci. Forum, 152–153 (1994) 13.

[6] J.M. Tarascon and D. Guyomard, J. Electrochem. Soc., 138 (1991) 2864; D. Guyomard and J.M. Tarascon, J. Electrochem. Soc., 139 (1992) 937.

[7] K.A. Striebl, C.Z. Deng, S.J. Wen and E.J. Cairns, J. Electrochem. Soc., 143 (1996) 1821.

[8] F.K. Shokoohi, J.M. Tarascon, B.J. Wilkens, D. Guyomard and C.C. Chang, J. Electrochem. Soc., 139 (1992) 1845.

[9] J. McBreen, Electrochim. Acta, 20 (1975) 221.

[10] A. Kozawa, in K.V. Kordesch (ed.), Batteries, Vol. 1, Manganese Dioxide, Marcel Dekker, New York, 1974, p. 385.

[11] H. Kahil, J. Phys. Cond. Matter, 17 (1995) 3227.